

Generation-Aware Electrified Production: Application to a Batch Evaporator for the Synthesis of TiO₂ Nanoparticles

Filippo Tamagnini*, Sebastian Engell

Technische Universität Dortmund, Emil-Figge Straße 70, Dortmund

filippo.tamagnini@tu-dortmund.de

This contribution addresses the problem of optimizing the operation of a batch process where energy is supplied electrically from mixed traditional and renewable sources. The case study considered here is that of an evaporator for the synthesis of titanium dioxide nanoparticles, where an energy-demanding distillation step is optimized and scheduled taking into account the forecasted availability of energy from renewables. The goal is to optimize the utilization of the energy from the renewable sources, without violating process and product constraints. A method is outlined to assess whether predictive demand-side management is a viable option and how to integrate it into the operation of a batch process based on the process characteristics.

1. Introduction

One of the measures that are necessary to mitigate climate change is to decrease the carbon intensity of the industrial and energy sectors. This requires, among other things, to increase the amount of energy supplied from renewable sources, while at the same time cutting down on the use of fossil fuels (IPCC, 2014). The electrification of the chemical and process industry can have a substantial impact, due to the energy-intensive nature of many unit operations. While on one hand, a large portion of the energy used in these sectors is in the form of heat, on the other the number of technologies for the electrification of traditional processes is increasing. Furthermore, electrical heating is already a valid technological solution for many medium and small productions due to the technical and operational simplicity of the equipment, and when electricity is supplied by renewable sources, its carbon intensity significantly decreases (Madeddu et al., 2020).

Renewable energy sources like solar and wind are among the best candidates to power the energy transition, although they are characterized by intermittency and non-dispatchability. In other words, their output changes more or less predictably during the day and across seasons without being able to control it. These characteristics can be problematic when integrating them in the energy mix, as they require the end users to make up for the lack of flexibility from the supply side. This can deter investments in renewable energy generation, due to the risk of not being able to exploit the installed capacity at its maximum potential (Egli, 2016). The process industry, however, can provide the necessary flexibility to ensure a functional integration of non-dispatchable energy sources. Batch processes can be very useful in this regard, as their energy consumption envelope is peaked in its nature and can be modified in different ways to match the times of the availability of renewable energy availability. The goal of this contribution is to showcase how this flexibility can be exploited to make better use of available renewable sources and to summarize the requirements for this to be possible.

2. Description of the process

The process used as case study is the synthesis of titanium dioxide nanoparticles. In this process, a suspension of nanoparticles is driven towards an equilibrium particle size distribution, which depends on the composition of the suspension and its temperature (Vorkapic and Matsoukas, 2005). The process occurs over a time window of six hours, and it essentially involves the distillation of a byproduct of the reaction. The plant consists of an electrically heated reaction vessel that is coupled to an overhead vapor condenser. The vessel is initially loaded with a mixture of water and titanium isopropoxide (precursor). The precursor is hydrolyzed by water and generates a pool of titanium dioxide primary particles and an alcoholic byproduct that is miscible in water. A

distribution of aggregates of different particle sizes is produced as a result of agglomeration and deagglomeration processes. The byproduct of reaction promotes the agglomeration process and as a result, the forming of larger aggregates. In order to obtain a particle population with smaller sizes, the alcohol needs to

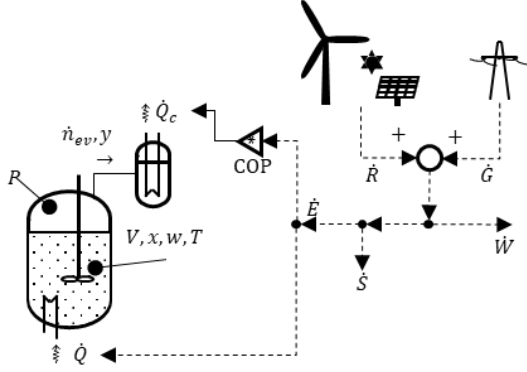


Figure 1: process diagram for the case study. The dashed lines represent electrical connections with the power sources. The arrows denote the direction of flow of energy.

be evaporated under vacuum. The heating power $\dot{Q}(t)$ and the evaporator pressure $P(t)$ are manipulated to control the process. A mathematical model of the process consisting of mass and energy balances, the vapor-liquid equilibrium equations and the moment balance equations of the particle size distribution was developed and presented in previous work. The state of the system is given by the moles of water and alcohol in the liquid phase, the temperature of the liquid, the moments of the particle size distribution and the fraction of alcohol bound to the surface of the aggregates. The model is compactly represented by using the state vector $\mathbf{x} = (n_W, n_A, T, \mu_0, \dots, \mu_{N-1}, S)^T$. From the moments, it is possible to compute an average particle size $Z = Z(\mu_0, \dots, \mu_{N-1})$ which is used to characterize the product quality. The vector $\mathbf{u} = (\dot{Q}, P)^T$ is referred to as the input vector. The evolution of the system is described by a set of differential equations $\dot{\mathbf{x}} = \mathbf{f}(\mathbf{x}, \mathbf{u})$. The instantaneous electrical power consumption of the process outlet $\dot{E} = \dot{E}(\mathbf{x}, \mathbf{u})$ is the

sum of the heat input to the evaporator and the electrical power necessary to condense the vapor at the process conditions. The condenser operates with a coefficient of performance COP, that is the ratio of the heat removed by the condenser to the supplied electrical energy. A schematic diagram of the process is shown in Figure 1, where the electrical connections are also shown.

The power generation is split among a renewable generator \dot{R} (non dispatchable and with finite capacity) and the grid \dot{G} (flexible). The energy consumption is split among the process and one additional sink \dot{S} , that reflects the ability to make use of the residual generation from renewables. Any excess power generation (\dot{W}) is wasted.

3. Economic optimization of the process

The goal of the optimization is to schedule and to control the process such that an economic cost function J is minimized, and constraints are satisfied. The process is controlled by modifying the input variables over time within specified hard bounds (trajectory optimization) and by manipulating the starting time of the batch (process scheduling).

$$\min_{\mathbf{u}(t), \mathbf{x}(t), t_0} J = \int_{t_0}^{t_0 + \Delta t} \phi(\mathbf{x}(t), \mathbf{u}(t), t) dt \quad \text{subject to:} \quad (1-a)$$

$$\frac{d\mathbf{x}}{dt} = \mathbf{f}(\mathbf{x}, \mathbf{u}) \quad \text{for all } t_0 \leq t \leq t_f \quad (1-b)$$

$$\mathbf{x}(t_0) = \mathbf{x}_0 \quad (1-c)$$

$$\mathbf{u}_{\min} \leq \mathbf{u}(t) \leq \mathbf{u}_{\max} \quad \text{for all } t_0 \leq t \leq t_f \quad (1-d)$$

$$t_{0,\min} \leq t_0 \leq t_{0,\max} \quad (1-e)$$

$$\mathbf{0} \leq \mathbf{C}(\mathbf{x}(t), \mathbf{u}(t)) \quad \text{for all } t_0 \leq t \leq t_f \quad (1-f)$$

$$\mathbf{0} \leq \mathbf{C}_f(\mathbf{x}(t_0 + \Delta t), \mathbf{u}(t_0 + \Delta t)) \quad (1-g)$$

In the case of the nanoparticle synthesis, a terminal constraint (\mathbf{C}_f) is used to enforce the quality of the product at the end of the process. One suitable choice as economic indicator is the total cost of energy of the process, and is obtained by setting $\phi(\mathbf{x}, \mathbf{u}, t) = EP(t) \cdot \dot{E}(\mathbf{x}(t), \mathbf{u}(t))$, where $EP(t)$ is the energy price at time t and $\dot{E}(\mathbf{x}, \mathbf{u})$

the electrical power consumption of the process. If energy is available at a constant price, then the optimal control policy is the one that minimizes the total energy consumption, and the starting time is irrelevant. In practice however, energy can be available at a variable price for several reasons, for example if the plant operator participates in demand-side management programs (Palensky and Dietrich, 2011) or if it can source its energy from an in-house available generator. In Tamagnini and Engell (2022), one scenario was considered where the starting time of the process was fixed and electrical power from a renewable source was available at a discounted price inside a predicted time window, with unlimited capacity and no restrictions on its use. In this work, the case where the renewable generator is subject to capacity constraints is investigated, explicitly taking into account the possibility to recover the leftover capacity. Let $\hat{R}(t)$ be the renewable power capacity at time t . It is assumed that the power from the renewable source can be absorbed at zero price from the renewable source until depletion, while the electrical grid supplies the remainder at a constant price EP. Once the process trajectory has been established, the power consumption from the grid $\hat{G}(t)$ is given by the following relationship:

$$\hat{G} = \begin{cases} \dot{E} - \hat{R}, & \hat{R} \leq \dot{E} \\ 0, & \text{otherwise} \end{cases} \quad (2)$$

The difference $\hat{R} - (\dot{E} - \hat{G})$ is the residual renewable capacity after the allocation of the process. This capacity can be used to generate an additional revenue (for example by reselling it to the grid or to power other processes in the plant) or savings (e.g. by storing the excess energy in a battery). This opportunity is modeled by means of a simple rule. Let \hat{L} be the maximum level of residual capacity that can be utilized. The recovered capacity \hat{S} is calculated as follows (the residual capacity is consumed to the maximum possible extent):

$$\hat{S} = \begin{cases} \hat{R} - (\dot{E} - \hat{G}), & \hat{R} - (\dot{E} - \hat{G}) \leq \hat{L} \\ \hat{L}, & \text{otherwise} \end{cases} \quad (3)$$

The difference $\hat{W} = \hat{R} - (\dot{E} - \hat{G}) - \hat{S}$ is the wasted renewable capacity.

The economic performance indicator to minimize is the total cost of the energy supplied by the grid for the first process minus the earnings made by recovering the residual capacity:

$$J = EP \int_{t_0}^{t_0+\Delta t} \hat{G}(x(t), \mathbf{u}(t), t) dt - RP \int_{t_0}^{t_0+\Delta t} \hat{S}(x(t), \mathbf{u}(t), t) dt \quad (4)$$

Where RP is the value of the recovered energy from renewable sources (recovery price, that similarly to the electricity price is constant throughout the process time window).

A model for the renewable capacity as a function of time is assumed as coming from a solar panel installation as the renewable generator, and is modelled using the following expression:

$$\hat{R}(t) = \frac{A}{1-b} \max\left(0, \cos\left(2\pi \frac{t-12}{24}\right) - b\right) \quad (5)$$

The term A is the apex power generation at $t = 12$. The term b is an offset parameter that increases or decreases the hours of renewable generation. These are related to b as: $t_{\hat{R}} = \frac{24}{\pi} \cos^{-1} b$.

Two solution approaches are now considered: one where the trajectory of the process is fixed and one where the full optimization problem (including the trajectory of the process) is solved.

3.1 Optimal scheduling of the process – fixed trajectory

In this approach, only the starting time t_0 of the process is scheduled, a precomputed input trajectory $\mathbf{u}(t) = \mathbf{u}^*(t - t_0)$ is applied to the process. The input is assumed to be the one that minimizes the overall energy consumption of a batch under the constraints stated above. The resulting trajectory of the process, and hence the power consumption profile $\dot{E}(t) = \dot{E}^*(t - t_0)$ can be used to compute the cost function (4) as a function of t_0 only. The resulting optimization problem is nonlinear and there are multiple and equivalent solutions under certain circumstances. Furthermore, the cost function may be nonconvex, depending on the exact shape of the capacity profile or the power consumption profile. Given the simplicity of the problem, rather than using a gradient based search, it is possible to solve the problem by discretizing the solution space, evaluating the cost function for all the values of t_0 , and selecting the solution based on the cost and some additional criteria, for example choosing the minimum t_0 that results in the minimum cost.

3.2 Optimal scheduling of the process – flexible trajectory

In this approach, both the starting time of the process, t_0 and the input $\mathbf{u}(t)$ are optimized. The variables are discretized in time on finite elements and collocation points. For this work, the input was parameterized by a piecewise linear continuous function. The resulting trajectory is the solution of the differential equation (1-b).

The problem was implemented in Python using the automatic differentiation toolbox “CasADi” (Andersson et al, 2019), using IPOPT as optimizer (Wächter and Biegler, 2006). In order to be able to consider the variable starting time, the limits of integration in the cost function were replaced with 0 and Δt , and the time variable was substituted with $t = t^* + t_0$. It should be mentioned that the problem is still nonconvex and can still admit multiple (equivalent) solutions. Additional criteria can be specified in the cost function as small additive penalties, such as a cost dependent on the starting time to privilege earlier starting times.

As a concluding remark to this section, the strengths and weaknesses of the two approaches are highlighted. From a purely practical standpoint, the former is more easily applicable. The trajectory to be applied needs not to be obtained by optimization, but may be established by practice. This makes it possible to use it even when very limited knowledge about the process is available (in fact, the power consumption profile is the only piece of information necessary for it to be used). On the other hand, if the profile of the generation capacity is significantly different from the one of the power consumption, the second approach is able to use the available capacity more effectively, as shown in the power profiles in Figure 2.

4. Results and discussion

The optimization was carried out for several combinations of the parameters $A > 0$, $b \geq 0$, $\dot{L} \geq 0$ and $RP/EP \leq 1$. The maximum possible power consumption of the process is 13.3 kW (not encountered in practice) when both the condenser and the evaporator operate at full power. The energy-optimal trajectory was used in the fixed trajectory approach. To summarize the solutions resulting from the two approaches, the grid energy percentage, renewable energy percentage and process cost percentage relative to the total energy use of the energy-optimal solution are defined:

$$\text{Grid energy } \%_{E.O.} = 100 \cdot \frac{\int \dot{G}(t)dt \text{ [Current solution]}}{\int \dot{E}(t)dt \text{ [Energy optimal]}} \quad (6)$$

$$\text{Renewable energy } \%_{E.O.} = 100 \cdot \frac{\int \dot{R}(t)dt \text{ [Current solution]}}{\int \dot{E}(t)dt \text{ [Energy optimal]}} \quad (7)$$

$$\text{Process cost } \%_{E.O.} = 100 \cdot \frac{J \text{ [Current solution]}}{EP \cdot \int \dot{E}(t)dt \text{ [Energy optimal]}} \quad (9)$$

The sum of the grid and renewable energy provision percentages can be larger or equal than 100 and denotes the total energy consumption of the solution relative to the energy optimal solution. The process cost is expressed relative to the energy optimal solution and to the grid energy price. Based on the ability of the renewable source to sustain the energy-optimal solution in its entirety and the ability to recover the residual generation capacity, four cases are identified.

4.1 The renewable source is sufficient to sustain the energy-optimal trajectory entirely and it is possible to recover the residual capacity entirely

As long as $RP \leq EP$, the flexible trajectory approach solution coincides with the energy-optimal one, because any variation in the power profile leads to an increased power consumption and therefore a reduction in the recoverable power. Multiple starting times are possible as long as the energy consumption profile of the process remains below the renewable generation curve.

4.2 The renewable source is sufficient to sustain the energy-optimal trajectory entirely and it is not possible to recover the residual capacity entirely

In this scenario, the renewable generation is sufficient to sustain the process entirely, and the residual capacity is more than can be recovered. Slight advantages could still be achieved, in theory, if the recovered capacity could be increased: that is, if there are points in time where the residual capacity after the process is less than the recovery capacity ($0 < \dot{S}(\tau) < \dot{L}$, for some τ in the process time window). In such cases, the profit of the process could be increased by means of the flexible trajectory approach. In practice, however, the improvement was found to be marginal in all the considered cases ($|\Delta \text{Energy cost } \%_{E.O.}| < 1\%$).

4.3 The renewable source is insufficient to sustain the energy-optimal trajectory entirely and it is possible to recover the residual capacity entirely

If the energy-optimal power trajectory cannot be supplied by the renewable source entirely, it may be more profitable to operate the process less efficiently (with a higher energy consumption than the energy-optimal and at the expense of a reduced recovered capacity), such that the consumption of grid power is reduced.

The extent of the tradeoff is determined by the ratio RP/EP . In practice, however, only for very low values of RP/EP the flexible trajectory solution was found to improve the profit, as summarized in Table 1, for $A = 5$, $b = 0.4$ and $\dot{L} = 5$.

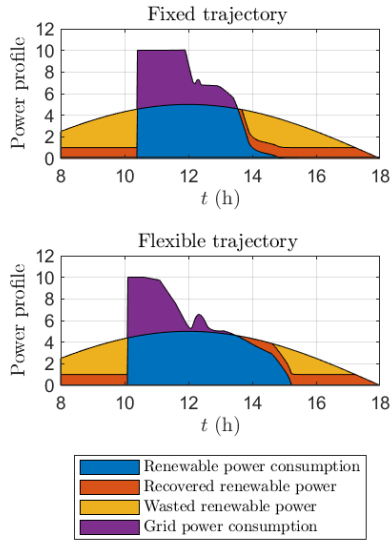


Figure 2: Comparison of the power profile resulting from the fixed trajectory approach and the one resulting from the flexible trajectory approach for the scenario described in 4.4, with $A = 5$, $b = 0.0$, $\dot{L} = 1$ and $RP/EP = 0.3$.

Table 1: Comparison of the optimal process cost percentage for the fixed and the flexible trajectory approaches for different values of the recovery price for the scenario described in 4.3.

RP/EP	Process cost % _{E.O.} (fixed trajectory)	Process cost % _{E.O.} (flexible trajectory)	Diff.
0.0	40.4	32.2	-8.2
0.3	27.4	25.0	-2.4
0.5	18.8	18.7	-0.1
0.7	10.1	10.1	0.0
1.0	-2.9	-2.9	0.0

Table 2: Comparison of the optimal process cost percentage for the fixed and the flexible trajectory approaches for different values of the recovery price for the scenario described in 4.4.

RP/EP	Process cost % _{E.O.} (fixed trajectory)	Process cost % _{E.O.} (flexible trajectory)	Diff.
0.0	39.3%	29.5%	-9.8%
0.3	32.4%	24.6%	-7.8%
0.5	27.8%	22.5%	-5.3%
0.7	23.2%	17.7%	-5.5%
1.0	16.2%	11.0%	-5.2%

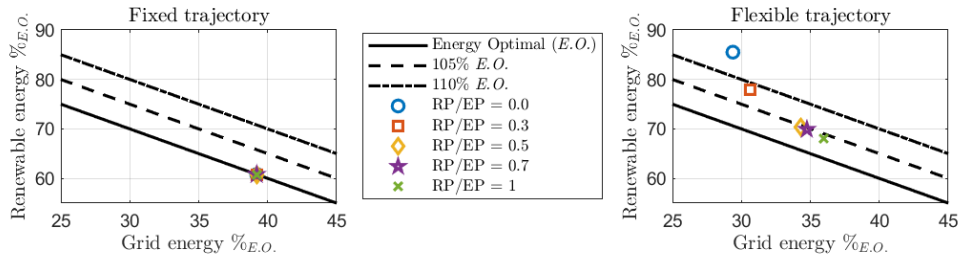


Figure 3: Comparison of the grid and renewable energy provision percentages for the fixed and flexible approaches, for different values of the recovery price to energy price ratio for the scenario described in section 4.4. All the points are calculated with $A = 5$, $b = 0$ and $\dot{L} = 1$. The diagonal lines denote points with the same total energy consumption. The solid black line corresponds to a total energy consumption equal to the one of the energy-optimal solution. The cost for each solution is given in Table 2.

4.4 The renewable source is insufficient to sustain the energy-optimal trajectory and it is not possible to recover the residual capacity entirely

In this case, the flexible trajectory approach can actually lead to a measurable improvement of the cost upon the fixed trajectory approach, even when the residual power can be recovered with $RP/EP \sim 1$, as shown in Table 2 for $A = 5$, $b = 0.0$ and $\dot{L} = 1$. As expected, the solutions of the flexible trajectory optimization use more energy overall than the fixed trajectory ones. This is visible in the second plot of Figure 3, where the two approaches are compared in terms of relative energy use. The recovery price determines how much the flexible trajectory solution departs from the fixed trajectory one. The increased energy consumption, however comes with a reduction of the power consumed from the grid and an increased renewable power use. Furthermore, the wasted renewable capacity is reduced, compared to the fixed trajectory approach, as visible in Figure 2.

5. Conclusions and further work

In this work it was outlined how process scheduling and trajectory optimization can be used in combination to adapt the operation of a process to the availability of renewable power, and some examples of the features that

the solutions possess were provided. The main takeaways are that, when the renewable capacity is limited, further reductions in the consumption of grid power can be obtained by adapting the trajectory of the process accordingly, and this is especially true when there is a limited ability to recover the residual capacity.

In the situation where there is an excess of renewable generation or when the plant is flexible enough to consume power at its maximum potential, scheduling the process operated with the energy-optimal trajectory is already sufficient in reducing the reliance on grid power and can be used by the plant operator to easily integrate the renewable generation.

Both approaches can be thought of as predictive demand-side management practices. The schedule or trajectory can be computed in advance based on seasonal values of the renewable capacity, although if a forecast is available for the generation capacity, it is also possible to optimize the trajectory on a day-by-day basis.

Other demonstrations of predictive demand side management exist in the literature, such as Kelley et al., 2020, however they use the market price of energy as driver for the optimization. While from an economic standpoint this is the best approach, in practice it would only be relevant for enterprises that can directly participate in the electricity market, thus limiting its applicability. Explicitly taking the renewable generation into account, on the other hand, makes the practice accessible for small and medium enterprises as well and can lead to a greater impact on the overall energy consumption patterns. Nonetheless, the methods presented here can be extended with minor effort to situations where different energy tariffs are available at different times of the day.

As a concluding remark, it is to be pointed out that the problem solved in this work is a “toy problem” in comparison to real-world scheduling problems, where a number of processes have to be allocated under stringent sequencing and production constraints. In other words, the scenario considered here benefits from a high flexibility with respect to timing. It can be assumed, that when this flexibility is reduced and the process is locked into place time-wise, then the trajectory optimization will play a more important role in making the best use of the available renewable generation capacity.

Nomenclature

A – Renewable power generation at solar apex, kW	\dot{L} – Maximum recoverable residual capacity, kW
b – Renewable power generation offset, -	\dot{R} – Renewable generation capacity, kW
\dot{E} – Electrical power consumption of the process, kW	RP – Recovery price for the residual capacity, €/kWh
EP – Grid energy price, €/kWh	\dot{S} – Recovered residual capacity, kW
\dot{G} – Grid power consumption, kW	\dot{W} – Wasted renewable capacity, kW

Acknowledgments

The project leading to this publication has received funding from the European Union’s Horizon 2020 research and innovation programme under grant agreement No. 820716 (SIMPLIFY).

References

- Andersson J., Gillis J., Horn G., Rawlings J. B., Diehl M., 2019, CasADi – A software framework for nonlinear optimization and optimal control, *Mathematical Programming Computation*, 11, 1-36
- Egli F., 2020, Renewable energy investment risk: an investigation of changes over time and the underlying drivers, *Energy Policy*, 140, 6–9.
- IPCC, 2014: Climate Change 2014: Synthesis Report. Contribution of Working Groups I, II and III to the Fifth Assessment Report of the Intergovernmental Panel on Climate Change [Core Writing Team, R.K. Pachauri and L.A. Meyer (eds.)]. IPCC, Geneva, Switzerland, 99-100
- Kelley M. T., Baldick R., Baldea M., 2020: An empirical study of moving horizon closed-loop demand response scheduling, *Journal of Process Control*, 92, 137-148
- Madeddu S., Ueckerdt F., Pehl M., Peterseim J., Lord M., Kumar K. A., Krüger C., Luderer G., 2020, The CO₂ reduction potential for the European industry via direct electrification of heat supply (power-to-heat), *Environmental research letters*, 15, 2-9
- Palensky P., Dietrich D., 2011: Demand Side Management: Demand Response, Intelligent Energy Systems, and Smart Loads, *IEEE Transactions on industrial informatics*, Vol. 7, No. 3, 381-382
- Tamagnini F., Engell S., 2022, Optimal operation of a batch evaporator for the controlled production of titania nanoparticles, *Computer Aided Chemical Engineering*, 51, 499-504
- Vorkapic D., Matsoukas T., 2005, Effect of Temperature and Alcohols in the Preparation of Titania Nanoparticles from Alkoxides, *Journal of the American Ceramic Society*, 159, 1-6
- Wächter A., Biegler L., 2006: On the implementation of an interior-point filter line-search algorithm for large-scale nonlinear programming, *Mathematical Programming*, 106, 25-57